L132

Effect of Frequency Ratio on the Force Coefficients of a Cylinder Oscillated in a Uniform Stream

László Baranyi[1]

[1]Department of Fluid and Heat Engineering, University of Miskolc, Hungary,
arambl@uni-miskolc.hu

Keywords: Circular cylinder, Oscillating cylinder, Frequency ratio, Low Reynolds number flow

Abstract: A finite difference solution is presented for 2D low Reynolds number flow around a circular cylinder placed in a uniform flow. The cylinder is oscillated in-line or transversely or is moved along an elliptical path. Abrupt jumps between two state curves were found in the time-mean (TM) and root-mean-square (rms) values of the force coefficients under lock-in conditions when plotted against frequency ratio. For orbital cylinder motion, jumps were found at certain frequency ratio values in the TM and rms values of all force coefficients and number and location of jumps were identical for all coefficients, similar to previous results plotted against ellipticity. When the cylinder was oscillated in-line, sudden changes were found only for the TM of lift and torque coefficients. However, when the cylinder was oscillated in transverse direction only, none of the TM and rms curves showed any jumps. Pre- and post-jump analysis (flow patterns, limit cycle curves) revealed switches in vortex structure.

1. Introduction

The near-wake structure of bluff bodies is very rich in complex phenomena in any case, but especially when the body is in motion. Lu and Dalton (1996) and Blackburn and Henderson (1999), in their studies of a transversely oscillating cylinder, found sudden switches in vortex structure at two different frequency ratio values. An experimental study by Williamson and Roshko (1988) led to a wake mode map showing different vortex shedding domains for transverse cylinder motion.

For the even more complex case of combined transverse and in-line motion that leads to a cylinder tracing an orbital path, switches have also been identified. It has been found that when a cylinder orbits in a uniform flow at low Reynolds number (Re=Ud/v), its flow structure changes abruptly at certain values of orbital ellipticity. There appear to be two states between which the solution switches. The two state curves can be reached in different ways such as using different ellipticity values (Baranyi, 2004) or changing the initial position of the cylinder (Baranyi, 2008).

This paper reports on a systematic investigation of the effect of frequency ratio on vortex shedding. Didier and Borges (2006) surveyed flow around cylinders in motion over a wide cylinder oscillation frequency domain (although orbital motion was limited to a fully circular path) and identified lock-in domains. Here, a detailed study in a relatively small frequency domain is carried out for a cylinder following an orbital path, in in-line oscillation, and in transverse oscillation under lock-in condition.

2. Governing equations

The dimensionless governing equations for an incompressible constant property Newtonian fluid flow around an orbiting circular cylinder are the Navier-Stokes equations, the continuity equation and pressure Poisson equation written in a non-inertial system fixed to the cylinder (using standard notations):

$$\frac{\partial u}{\partial t} + u\frac{\partial u}{\partial x} + v\frac{\partial u}{\partial y} = -\frac{\partial p}{\partial x} + \frac{1}{\text{Re}}\nabla^2 u - a_{0x}, \qquad (1)$$

$$\frac{\partial v}{\partial t} + u\frac{\partial v}{\partial x} + v\frac{\partial v}{\partial y} = -\frac{\partial p}{\partial y} + \frac{1}{\text{Re}}\nabla^2 v - a_{0y}, \qquad (2)$$

$$D = \frac{\partial u}{\partial x} + \frac{\partial v}{\partial y} = 0, \qquad (3)$$

$$\nabla^2 p = 2\left[\frac{\partial u}{\partial x}\frac{\partial v}{\partial y} - \frac{\partial u}{\partial y}\frac{\partial v}{\partial x}\right] - \frac{\partial D}{\partial t}. \qquad (4)$$

The continuity equation is satisfied at every time step.

No-slip boundary condition is used on the cylinder surface for the velocity and a Neumann-type condition is used for pressure p. Potential flow is assumed far from

the cylinder. Boundary-fitted coordinates are used to impose the boundary conditions accurately. The domain, equations and boundary conditions are transformed to a computational plane. The transformed equations are solved by using the finite difference method. The Poisson equation for pressure is solved by the SOR method. For further details see Baranyi (2003, 2008). The 2D code developed by the author has been extensively tested against experimental and computational results (Baranyi, 2008) with good agreement being found. For this study the dimensionless time step was 0.0005 and the number of grid points 301x177. The ratio of the radius of the outer computational domain and cylinder radius was 40.

Figure 1 shows the flow arrangement. The motion of the centre of the cylinder with unit diameter is specified as follows:

$$x_0(t) = A_x \cos(2\pi f t); \quad y_0(t) = -A_y \sin(2\pi f t) \quad (5)$$

where $f_x = f_y = f$ and A_x, A_y are the dimensionless frequencies and amplitudes of cylinder oscillations in x and y directions, respectively. The negative sign in y_0 in equation (5) makes the cylinder orbit clockwise. Here for nonzero A_x, A_y amplitudes gives an ellipse, shown in the dotted line in Figure 1. A_y with $A_x=0$ yields pure transverse oscillation, A_x with $A_y=0$ yields pure in-line oscillation, and then as A_y is increased, the ellipticity $e=A_y/A_x$ increases to yield a full circle at $e=1$. When both amplitudes are zero the cylinder becomes stationary.
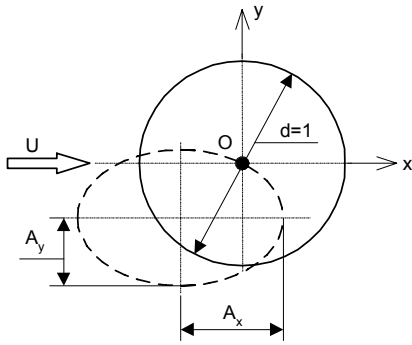

Figure 1. Layout for the orbital path of the cylinder

3. Computational results

3.1. State curves and initial results

Earlier computations investigated the time-mean (TM) value and root-mean-square (rms) values of force coefficients (lift C_L, drag C_D, base pressure coefficients C_{pb}, torque coefficient t_q) for an orbiting cylinder in a uniform flow. Abrupt jumps were found when these values were plotted against ellipticity e, with Re, A_x and f kept constant (Baranyi, 2004; 2008). A typical example for the TM of lift is shown in Figure 2 for Re=160, $A_x=0.3$, $f=0.9St_0$, $St_0=0.1882$ (St_0 is the Strouhal number for a stationary cylinder at the given Re). Note that there are two roughly parallel state or envelope curves. In all computations made so far, C_{Lmean} and t_{qmean} have shown this pattern (subscript *mean* refers to time-mean values).

The location and number of jumps for the other force coefficients were identical with those shown in Figure 2,

but it was found that the location and number can vary with a change in initial condition Θ (the polar angle characterising the initial cylinder position, from which clockwise motion is initiated). The initial condition of $\Theta=0°$ (when the centre of the cylinder is on the positive x axis), was used in the case shown in Figure 2.
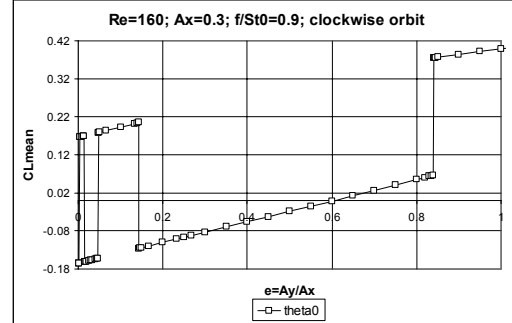

Figure 2. Time-mean value of lift versus ellipticity

The effect of initial condition is demonstrated in Figure 3, where it can be seen that the full state curves can be reproduced using three different initial conditions ($\Theta=60°$, 90° and 180°). Note that these are for the same set of parameters as in Figure 2, with the exception of initial condition. The existence of two state curves is clearly seen, showing that two potential solutions exist, and the actual solution switches between them (Baranyi, 2008).
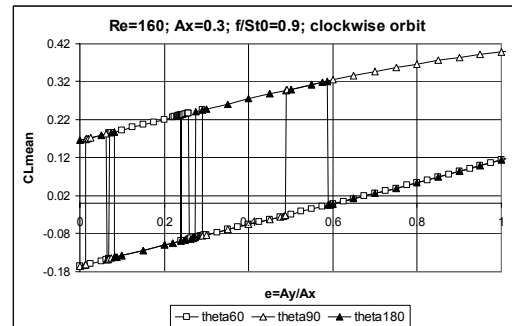

Figure 3. Time-mean value of lift versus ellipticity: effect of initial condition ($\Theta=60°$, 90° and 180°)

3.2. Orbital cylinder motion vs. frequency ratio

Next the effect of frequency ratio f/St_0 was investigated on the TM and rms values of force coefficients. Two sets of computations were carried out for an orbiting cylinder: (A) Re=160; $A_x=0.3$; $A_y=0.15$; $St_0=0.1882$; $\Theta=0°$; (B) Re=140; $A_x=0.4$; $A_y=0.2$; $St_0=0.1821$; $\Theta=0°$. Computations were repeated for different frequency ratios f/St_0 in the lock-in domain. It was found that when TM and rms values of force coefficients (C_L, C_D, C_{pb}, t_q) are plotted against f/St_0, jumps occurred in every curve. There seem to be two state curves between which the solution jumps, similar to results when plotted against ellipticity (Baranyi, 2008). The number and location of jumps are identical on each curve belonging to the same set of parameters. Curves were very similar to each other for sets A and B. Figures 4 and 5 show two curves for parameter set A.
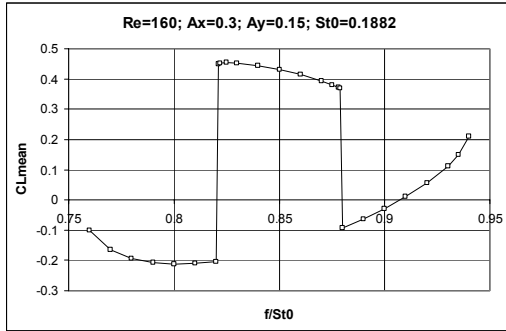
Figure 4. Time-mean value of lift versus frequency ratio
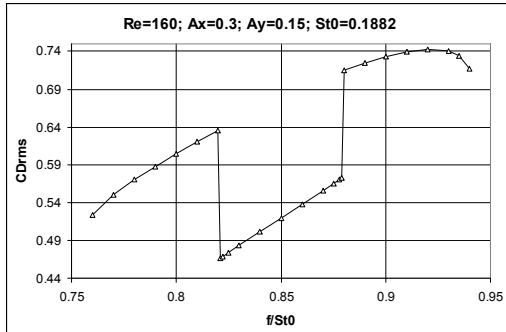

Figure 5. Rms value of drag versus frequency ratio

Pre- and post-jump analyses were carried out for the first jump in Figures 4 and 5. Figures 6 and 7 show the
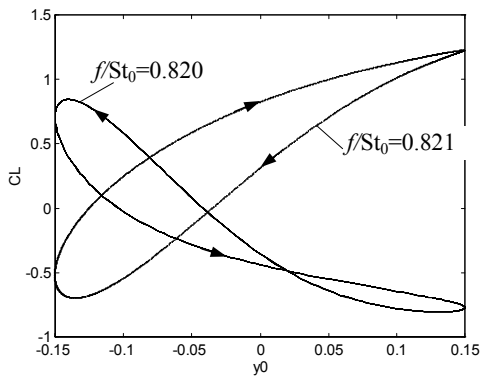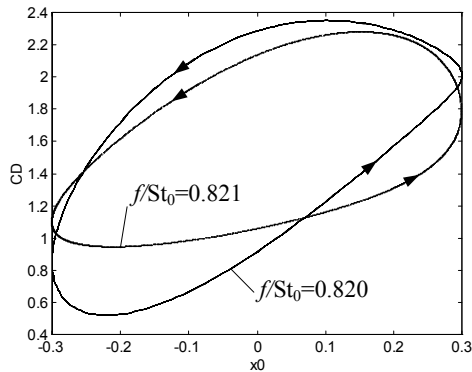

Figure 6. Limit cycle curve (y_0, C_L)

Figure 7. Limit cycle curve (x_0, C_D)

limit cycle curves for a pre-jump (f/St$_0$=0.820) and post-jump (f/St$_0$=0.821) frequency ratio for the limit cycles (y_0, C_L) and (x_0, C_D). It can be seen in Figure 6 that a tiny change in f/St$_0$ causes a drastic change in the

limit cycle curves, even changing the direction of orientation. The change in the limit cycle (x_0, C_D) (Figure 7) is less dramatic.

Contours of positive (black) and negative (grey) vorticity belonging to the uppermost cylinder position are given for pre-jump (a) and post-jump (b) cases in Figure 8. As seen in the figure, the flow patterns are essentially mirror images of each other. Note that the vortex shedding pattern is mode P, in which one pair of vortices is shed in a complete cycle (Williamson & Roshko, 1988).
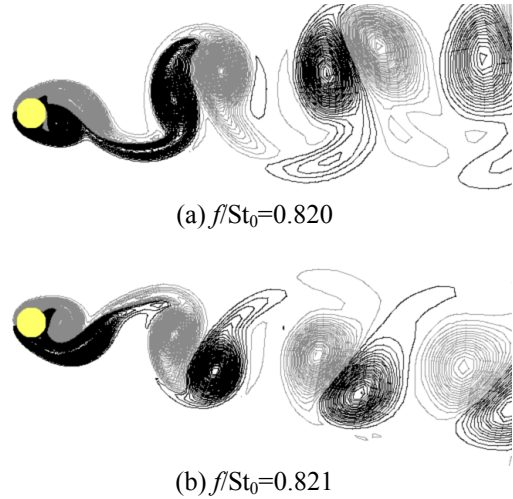

(a) f/St$_0$=0.820

(b) f/St$_0$=0.821

Figure 8. Vorticity contours for an orbiting cylinder (uppermost cylinder position) at two frequency ratios

3.3. In-line cylinder motion vs. frequency ratio

Investigations on in-line oscillation were carried out at parameter sets C (Re=160; A_x=0.3; St$_0$=0.1882; Θ=0°) and D (Re=140; A_x=0.4; St$_0$=0.1821; Θ=0°). TM and rms values plotted against f/St$_0$ showed jumps only in C_{Lmean} (Figure 9) and t_{qmean} (Figure 10), with matching location and number of jumps; for the other six curves no jumps were detected (an example is given in Figure 11).
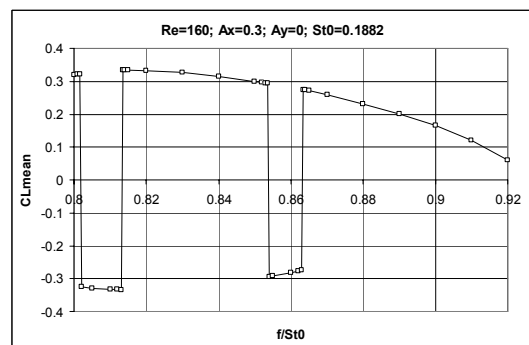

Figure 9. Time-mean of lift versus f/St$_0$

The TM values of C_L and t_q probably are distinguished from the rest because these are the only values which depend on whether the vortex is shed from the upper or lower side of the cylinder, meaning that they are T-periodic. All rms values and the TM values of C_D and C_{pb} are independent of the location of vortex shedding, so are T/2-periodic.
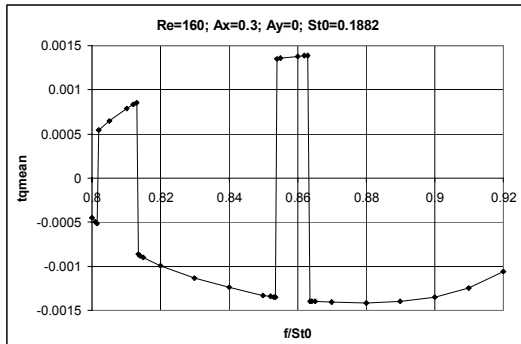
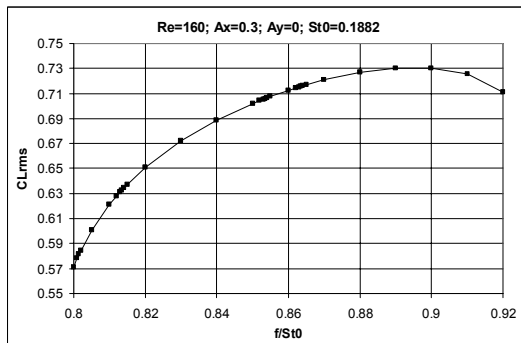Figure 10. Time-mean of torque coefficient versus f/St_0

Figure 11. Root-mean-square of lift versus f/St_0

Limit cycle curves for in-line oscillation are shown in Figure 12 for (x_0, C_L) at $f/\mathrm{St}_0=0.863$ (pre-jump) and 0.8635 (post-jump). The curves are near-mirror image and the direction of orientation changes with the jump. Limit cycle curves for (x_0, C_D) reveal no change at all through the jump in either shape or direction of orientation. Flow patterns were similar to those of orbital motion: a mirror image switch and mode P vortex shedding.
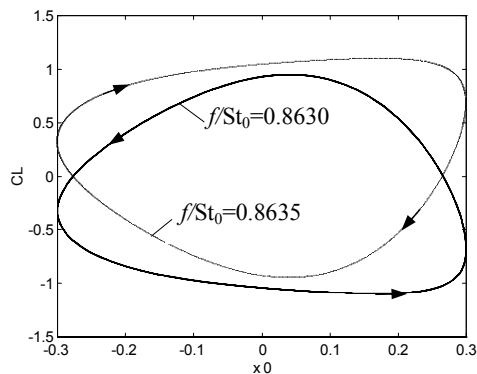

Figure 12. Limit cycle curve (x_0, C_L)

3.4. Transverse motion versus frequency ratio

As in the other cases, computations for a transversely oscillated cylinder were carried out for two sets of parameters, E (Re=160; A_y=0.3; St_0=0.1882; Θ=0˚) and F (Re=140; A_y=0.4; St_0=0.1821; Θ=0˚). Plotting TM and rms values against f/St_0 gave only continuous curves; no jumps were found at all in any of the force coefficients. The flow structure is 2S (two single vortices shed in one complete cycle) (Williamson & Roshko, 1988), giving the well-known Kármán vortex street (Figure 13).
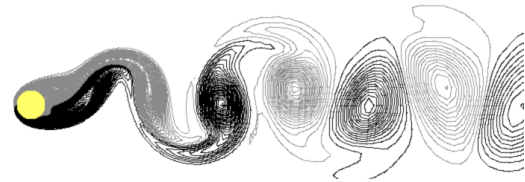

Figure 13. Vorticity contours for a transversely oscillating cylinder at f/St_0=0.88

4. Conclusions

This study investigates the effect of frequency ratio f/St_0 on vortex shedding at low Re for moving cylinders under lock-in condition. The TM and rms values of force coefficients were plotted against f/St_0 to identify jumps between state curves. Jumps were found in all cases for a cylinder in orbital motion; only for the TM of lift and the torque coefficient for in-line oscillation; and not at all for transverse oscillation. Pre-and post-jump analyses showed changes in shape and direction of orientation of limit cycles, especially for lift (orbital and in-line), and mirror image switches in flow patterns. Flow patterns for orbital and in-line motion were mode P, and mode 2S was found for transverse motion. Further investigation is planned, including the effect of switches in vortex shedding on energy transfer between cylinder and fluid.

5. Acknowledgements

6. References

Baranyi, L. 2003 Computation of unsteady momentum and heat transfer from a fixed circular cylinder in laminar flow. *Journal of Computational and Applied Mechanics*, Vol. 4, 13-25.

Baranyi, L. 2004 Sudden jumps in time-mean values of lift coefficient for a circular cylinder in orbital motion in a uniform flow. In *8th International Conference on Flow-Induced Vibration* (eds E. de Langre & F. Axisa), Paris, Vol. II, 93-98.

Baranyi, L. 2008 Numerical simulation of flow around an orbiting cylinder at different ellipticity values. *Journal of Fluids and Structures* (in press), doi: 10.1016/j.fluidstructs.2007.12.006

Blackburn, H.M. & Henderson, R.D. 1999 A study of two-dimensional flow past an oscillating cylinder. *Journal of Fluid Mechanics*, Vol. 385, 255-286.

Didier, E., & Borges, A.R.J. 2006 Numerical predictions of low Reynolds number flow over an oscillating circular cylinder. In *Conf. on Modelling Fluid Flow* (eds. T. Lajos & J. Vad), Vol. I, Budapest, 165-172.

Lu, X.Y. & Dalton, C. 1996 Calculation of the timing of vortex formation from an oscillating cylinder. *Journal of Fluids and Structures*, Vol. 10, 527-541.

Williamson, C.H.K. & Roshko, A. 1988 Vortex formation in the wake of an oscillating cylinder. *Journal of Fluids and Structures*, Vol. 2, 355-381.